

Cosmic evolution of scalar fields with multiple vacua: generalized DBI and quintessence

Changjun Gao*

*Key Laboratory for Computational Astrophysics, National Astronomical Observatories,
Chinese Academy of Sciences, Beijing, 100012, China and
State Key Laboratory of Theoretical Physics, Institute of Theoretical Physics,
Chinese Academy of Sciences, Beijing 100190, China*

You-Gen Shen†

*Shanghai Astronomical Observatory, Chinese Academy of Sciences, Shanghai 200030, China
(Dated: December 19, 2021)*

We find a method to rewrite the equations of motion of scalar fields, generalized DBI field and quintessence, in the autonomous form for *arbitrary* scalar potentials. With the aid of this method, we explore the cosmic evolution of generalized DBI field and quintessence with the potential of multiple vacua. Then we find that the scalars are always frozen in the false or true vacuum in the end. Compared to the evolution of quintessence, the generalized DBI field has more times of oscillations around the vacuum of the potential. The reason for this point is that, with the increasing of speed $\dot{\phi}$, the friction term of generalized DBI field is greatly decreased. Thus the generalized DBI field acquires more times of oscillations.

PACS numbers: 98.80.Es, 98.80.Cq

I. INTRODUCTION

Scalar fields play an important role in both theoretical physics and modern cosmology for their simple but non-trivial dynamics. In theoretical physics, they are present in the Jordan-Brans-Dicke theory as Jordan-Brans-Dicke scalar [1]; in Kaluza-Klein compactification theory as the radion [2]; in the Standard Model of particle physics as the Higgs boson [3]; in the low-energy limit of the superstring theory as the dilaton [4], tachyon [5] and DBI (Dirac-Born-Infeld) field [6]. In cosmology, scalar fields are employed to model the inflaton [7], the quintessence [8–14] (for a recent review of *quintessence*, see Refs. [15] and references therein), the k-essence [16, 17], the phantom [18], in order to drive the inflation of the early Universe or to speed up the expansion of the late Universe. We note that most of the scalar fields are hypothetical particles. But the Higgs Boson has uniquely been discovered by experiments.

Quintessence is a canonical scalar field which is assumed to be minimally coupled to gravity. Compared to other scalar fields, quintessence turns out to be the simplest scenario which is free of ghosts and instability problems. The dynamics of quintessence in the presence of matters has been studied in great detail for many different potentials [12–14, 19–28]. However, for a general quintessence potential, the equations of motion are rather involved. To our knowledge, one have not yet find a general method to write the equations of motion in the autonomous form for *arbitrary* potential. Thus the purpose

of this article is to report that we have found a way.

The DBI field describes the dynamics of D-branes evolving in a higher-dimensional warped spacetime. A novel aspect of this field is the existence of a speed limit on the field space, resulting from causality restrictions on the motion of the branes in the bulk spacetime. The speed limit is enforced by the non-canonical kinetic terms in the DBI field. This is different from the quintessence whose speed $\nabla\phi$ could be arbitrarily large. From this point of view, quintessence and DBI field are the counterpart of Newtonian and Special Relativity mechanics, respectively. The cosmic evolution of DBI field have been studied in Refs. [29]. These researches only apply to some special forms of potentials. Thus, to find a general method applying to *arbitrary* DBI potential constitutes the second purpose of this article.

II. GENERALIZED DBI FIELD

We consider a D3-brane with tension T evolving in a 5-dimensional spacetime. The dynamics of the mobile D3-brane is described by the DBI action. The D3-brane is free to move on the internal compact Calabi-Yau manifold. The generalized DBI action can be written as follows [6]

$$S = \int d^4x \sqrt{-g} \left[T(\psi) W(\psi) \sqrt{1 + \frac{1}{T(\psi)} \partial_\mu \psi \partial^\mu \psi} - T(\psi) + V(\psi) \right] + S_m. \quad (1)$$

Here $T(\psi)$ is the warped tension of the brane and S_m is the action for matters localized in the D3-brane. The potential $W(\psi)$ could arise under the condition that the

*Electronic address: gaojcj@bao.ac.cn

†Electronic address: ygshen@center.shao.ac.cn

brane is a non-BPS one [5] or there are multiple coincident branes [30]. The potential $V(\psi)$ is related to the brane's interactions with bulk fields or other branes.

In order to simplify our derivations, we define the variable ϕ as follows

$$\frac{1}{\sqrt{T(\psi)}}\partial_\mu\psi = \partial_\mu\phi. \quad (2)$$

Then above action can be written as

$$S = \int d^4x \sqrt{-g} \left[T(\phi) W(\phi) \sqrt{1 + \partial_\mu\phi\partial^\mu\phi} - T(\phi) + V(\phi) \right] + S_m. \quad (3)$$

Without the loss of physical significance, we could absorb the term $T(\phi)$ into $W(\phi)$ and $V(\phi)$, respectively. Then we find the action is simply

$$S = \int d^4x \sqrt{-g} \left[W(\phi) \sqrt{1 + \partial_\mu\phi\partial^\mu\phi} + V(\phi) \right] + S_m. \quad (4)$$

We shall investigate the cosmic evolution of the DBI field in the background of spatially flat Friedmann-Robertson-Walker Universe

$$ds^2 = -dt^2 + a(t)^2 (dr^2 + r^2 d\Omega^2), \quad (5)$$

where $a(t)$ is the cosmic scale factor. We model the matter sources present in the Universe as perfect fluids. The perfect fluids can be baryonic matter, relativistic matter and dark energy. We assume there is no interaction between the generalized DBI scalar field and the matter fields, other than by gravity. Then the Einstein equations and the equation of motion of the scalar field are given

$$\begin{aligned} 3H^2 &= \kappa^2 (W\gamma + V + \rho_m), \\ 2\dot{H} + 3H^2 &= -\kappa^2 (-W/\gamma - V + \omega_m \rho_m), \end{aligned} \quad (6)$$

and

$$\ddot{\phi} + \frac{1}{\gamma^2} \cdot 3H\dot{\phi} + \frac{1}{\gamma^3} \cdot \frac{V_{,\phi}}{W} + \frac{1}{\gamma^2} \cdot \frac{W_{,\phi}}{W} = 0, \quad (7)$$

respectively. Here $H \equiv \dot{a}/a$ denotes the Hubble parameter and dot is the derivative with respect to cosmic time, t . ρ_m and ω_m are the energy density and the equation of state for the matter sources. We have $\omega_m = -1, 0, 1/3, +1$ for the cosmological constant, dust matter, relativistic matter and stiff matter, respectively. In this paper, we shall consider the case of dust matter, $\omega_m = 0$. $V_{,\phi}$ and $W_{,\phi}$ denote the derivative with respect to ϕ . γ is defined by

$$\gamma = \frac{1}{\sqrt{1 - \dot{\phi}^2}}, \quad (8)$$

which has the physical meaning of the generalized Lorentz factor. It is apparent the speed of scalar $\dot{\phi}$ is

constrained to be smaller than the speed of light. This is remarkably different from the usual quintessence which could have arbitrary large speed in the sense of classical mechanics.

Observing Eqs. (6) and Eq. (7), we could absorb the constant $\kappa^2/3$ ($\kappa^2 = 8\pi$) into W, V and ρ_m , respectively,

$$W \longrightarrow W \cdot \frac{3}{\kappa^2}, \quad (9)$$

$$V \longrightarrow V \cdot \frac{3}{\kappa^2}, \quad (10)$$

$$\rho_m \longrightarrow \rho_m \cdot \frac{3}{\kappa^2}. \quad (11)$$

Then above equations of motion turns out to be

$$H^2 = W\gamma + V + \rho_m, \quad (12)$$

$$2\dot{H}/3 + H^2 = W/\gamma + V - \omega_m \rho_m, \quad (13)$$

$$\ddot{\phi} + \frac{1}{\gamma^2} \cdot 3H\dot{\phi} + \frac{1}{\gamma^3} \cdot \frac{V_{,\phi}}{W} + \frac{1}{\gamma^2} \cdot \frac{W_{,\phi}}{W} = 0. \quad (14)$$

Given the scalar potential $W(\phi)$, $V(\phi)$ and the equation of state ω_m , we are left with three variables, $a(t)$, ρ_m and the DBI field $\phi(t)$. Then we have three variables and three independent differential equations. So the system of equations is closed.

It is rather difficult to find the analytic solutions to the equations of motion (12-14). Hence in order to solve them numerically, we had better rewrite them in the autonomous form. To this end, we introduce the following dimensionless quantities

$$X \equiv \dot{\phi}, \quad U \equiv \frac{V_{,\phi}}{W^{\frac{3}{2}}}, \quad (15)$$

$$Y \equiv \frac{\sqrt{W}}{H}, \quad Q \equiv \frac{W_{,\phi}}{W^{\frac{3}{2}}}, \quad (16)$$

$$Z \equiv \frac{\sqrt{V}}{H}, \quad S \equiv \frac{V_{,\phi}}{V^{\frac{3}{2}}}, \quad (17)$$

$$N \equiv \ln a. \quad (18)$$

We see U, Q, S are the functions of DBI field, ϕ . So they can be expressed as the function of Y/Z . Now we have only three variables, namely, X, Y, Z and it is sufficient for us to derive the corresponding three independent differential equations. We remember that the system of equations of X, Y, Z are an autonomous system if and only if U, Q, S are expressed as the functions of X, Y, Z . For simplicity, we assume

$$\frac{V}{W} = \phi^2. \quad (19)$$

We emphasize that one could in general assume $V/W = F(\phi)$ with $F(\phi)$ other simple functions, for example, $F(\phi) = \phi^n, e^{\alpha\phi}, \ln\phi$ and so on. Then we could obtain $\phi = \phi(V/W) = \phi(Z/Y)$ from this equation. Similarly, U, Q, S could be expressed as the function of Z/Y .

Now with the aid of this assumption, we are able to write the Eqs. (12-14) in the autonomous form and deal with *any* scalar potential, $V(\phi)$ in the calculations. In this article, we shall focus on the scalar potential $V(\phi)$ with the expression of

$$V = V_0 + \frac{V_1}{\phi^6} (\phi - a_1)(\phi - a_2)(\phi - a_3) \cdot (\phi - a_4)(\phi - a_5)(\phi - a_6), \quad (20)$$

where V_i and a_i are all positive constants. The reason for this choice of potential is that what we want to study is a potential with multiple vacua. Scalar fields with multiple vacua are very interesting because they have both theoretical origin in string landscape [31] and theoretical study in Coleman-De Luccia tunnelling [32].

We note that the case of the well-known AdS throat, $W(\phi) = \lambda/\phi^4$ has been included in the desired one. As an example, we put $V_0 = 2$, $V_1 = 10^4$, $a_1 = 1$, $a_2 = 11/10$, $a_3 = 9/8$, $a_4 = 39/25$, $a_5 = 157/100$, $a_6 = 2$ in the following discussions.

In Fig. 1, we plot the potential $V(\phi)$ with respect to ϕ . There are two local maximum ($\xi_1 = 1.11$, $\xi_2 = 1.56$), one real vacuum ($\sigma_3 = 1.863$) and two false vacuum ($\sigma_1 = 1.029$, $\sigma_2 = 1.305$) for the potential. Physically, the scalar field would roll down the potential and then passes through the first (σ_1) and the second (σ_2) false vacuum. Finally, it arrives at the real vacuum (σ_3). The detail of the trajectory is closely related to the initial velocity, $\dot{\phi}_i$ (with the initial value, ϕ_i fixed). When the initial speed $\dot{\phi}_i$ is small enough, the scalar would acquire damped oscillations due to the Hubble friction in the first false vacuum and finally it is frozen in this vacuum. However, with the increasing of initial speed, the scalar could cross the first local maximum (ξ_1) and finally is frozen in the second false vacuum (σ_2). With even much larger initial velocity, the scalar could cross the two local maximum (ξ_1 and ξ_2) and finally dwells on the real vacuum (σ_3). Since the speed of the scalar is constrained to be smaller than the speed of light, the scalar can not climb the hill with arbitrary height. Due to the Hubble friction, we expect the fate of the scalar is to dwell on the real vacuum. In what follows, we shall show these points numerically.

Using the dimensionless variables defined in (15-18), the equations of motion (12-14) can be written in the following autonomous form

$$\begin{aligned} \frac{dX}{dN} &= -\frac{1}{\gamma^2} \cdot 3X - \frac{1}{\gamma^3} \cdot UY - \frac{1}{\gamma^2} \cdot QY, \\ \frac{dY}{dN} &= \frac{1}{2} QXY^2 - Y \frac{\dot{H}}{H^2}, \\ \frac{dZ}{dN} &= \frac{1}{2} SXZ^2 - Z \frac{\dot{H}}{H^2}, \end{aligned} \quad (21)$$

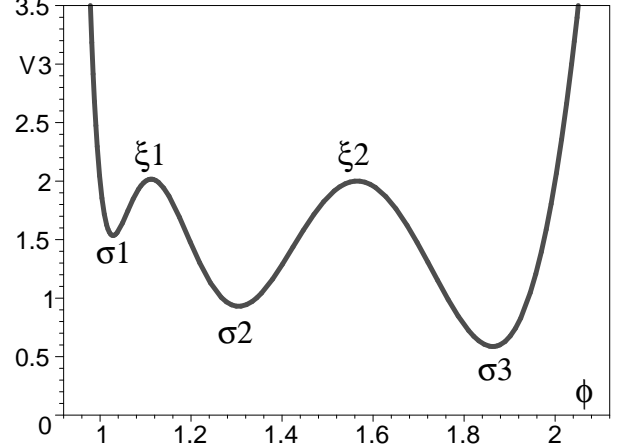


FIG. 1: The DBI potential $V(\phi)$ with respect to ϕ . There are two local maximum ($\xi_1 = 1.11$, $\xi_2 = 1.56$), one real vacuum ($\sigma_3 = 1.863$) and two false vacuum ($\sigma_1 = 1.029$, $\sigma_2 = 1.305$) for the potential. Physically, the scalar field would roll down the potential and then passes through the first (σ_1) and the second (σ_2) false vacuum. Finally, it arrives at the real vacuum (σ_3).

where U , Q , S are the functions of Y/Z and

$$\gamma = \frac{1}{\sqrt{1-X^2}}, \quad (22)$$

$$\frac{\dot{H}}{H^2} = 3Y^2 \cdot \frac{1-\gamma^2}{2\gamma} - \frac{3}{2} (1 - \gamma Y^2 - Z^2). \quad (23)$$

The Friedmann equation becomes the constraint equation

$$1 = \frac{Y^2}{\sqrt{1-X^2}} + Z^2 + \frac{\rho_m}{H^2}. \quad (24)$$

The equation of state w of the DBI scalar field is

$$w \equiv \frac{-1/\gamma - Z^2/Y^2}{\gamma + Z^2/Y^2}. \quad (25)$$

In Table I, we present the properties of the five fixed points for the scalar field. The points (a, c, e) correspond to the false vacua (σ_1 , σ_2) and real vacuum (σ_3). The three points are stable spirals. On these epoches, the scalar field behaves as a damping oscillator with the equation of state of firstly behaving as the dust matter and then oscillating approaching -1 (see Fig. (5)). The points (b, d,) correspond to the two local maximum (ξ_1 , ξ_2) and they are saddle points. On these points, the speed of the scalar field exactly vanishes and the DBI field acquires the equation of state of cosmological constant.

In Fig. (2-4), we plot the evolution of the speed, $\dot{\phi}$ of the generalized DBI field with ϕ . We fix the initial values

Name	X	Y	Z	ϕ	Stability	Ω_ϕ	w_ϕ
(a)	0	0.70	0.72	$\sigma_1 = 1.03$	Stable spiral (attractor)	1	-1
(b)	0	0.67	0.74	$\xi_1 = 1.11$	Saddle point	1	-1
(c)	0	0.61	0.79	$\sigma_2 = 1.31$	Stable spiral (attractor)	1	-1
(d)	0	0.54	0.84	$\xi_2 = 1.56$	Saddle point	1	-1
(e)	0	0.47	0.88	$\sigma_3 = 1.86$	Stable spiral (attractor)	1	-1

TABLE I: Properties of the critical points for the scalar potential given by Eq. (20).

of $\dot{\phi}$, ϕ and ρ_m/H^2 . By this way, the initial values of Y and Z are determined. Fig. (2) shows that when the initial speed $\dot{\phi}_i$ is small enough, the scalar would acquire damped oscillating due to the Hubble friction in the false vacuum (σ_1) and finally it is frozen in this vacuum. With the increasing of initial speed, the scalar crosses the first local maximum (ξ_1) and finally is frozen in the second false vacuum (σ_2) (see Fig. (3)). With even much larger initial velocity, the scalar crosses the two local maximum (ξ_1 and ξ_2) and finally dwells on the real vacuum (σ_3) (see Fig. (4)).

In Fig. (5), we plot the evolution of the equation of state w of the generalized DBI field corresponding to Fig. (4). We see the generalized DBI field previously behaves as the dust matter and then oscillating approaches -1 after a sufficient long time. The reason for oscillating of w can be understood as follows. Eq. (25) tells us when the speed of DBI field vanishes, the equation of state is -1 . Fig. (4) shows there are many times for the vanishing of speed during the damped oscillating. Every time the generalized DBI field acquires vanishing velocity, its equation of state is -1 .

III. QUINTESSENCE

In this section, we shall present the method for dealing with arbitrary quintessence potential. As an example, we would explore the cosmic evolution of quintessence field with multiple vacua. To this end, let's focus on the potential as follows

$$V = V_0 e^{b(\phi-a_1)(\phi-a_2)(\phi-a_3)(\phi-a_4)(\phi-a_5)(\phi-a_6)}, \quad (26)$$

where V_0 , b , a_i are positive constants. As an example, we consider, $V_0 = 1$, $b = 1$, $a_1 = 1/2$, $a_2 = 3/5$, $a_3 = 1$, $a_4 = 17/10$, $a_5 = 2$, $a_6 = 5/2$.

In Fig. 6, we plot the potential $V(\phi)$ with respect to ϕ . There are two local maximum ($\xi_1 = 0.813$, $\xi_2 = 1.862$), one real vacuum ($\sigma_3 = 2.342$) and two false vacuum ($\sigma_1 = 0.545$, $\sigma_2 = 1.355$) for the potential. Physically, the scalar field would roll down the potential and then damped oscillates between these vacua. Given an initial finite velocity $\dot{\phi}$ and field value ϕ_0 , the fate of the scalar is expected to dwell on the one of the vacuum due to the Hubble friction. In what follows, we shall show these points numerically.

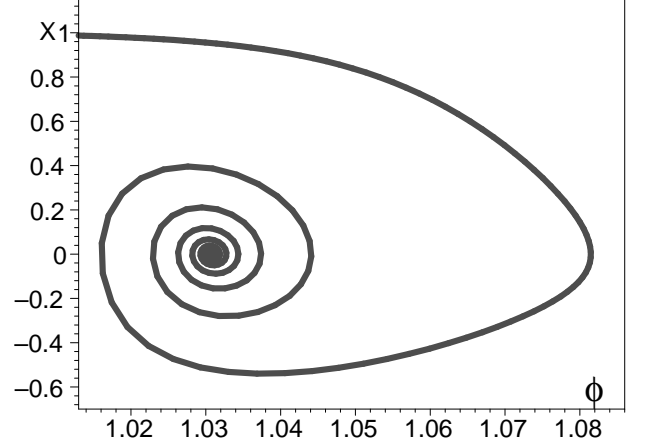


FIG. 2: Evolution of the speed ($X = \dot{\phi}$) of generalized DBI field with ϕ . The point ($\phi = \sigma_1 = 1.03$, $X = 0$) is a stable spiral and thus an attractor. In this case, the generalized DBI field behaves as a damping oscillator in the false vacuum (σ_1) and finally is frozen.

The Einstein equations and the equation of motion of the quintessence are given by

$$3H^2 = \kappa^2 \left(\frac{1}{2} \dot{\phi}^2 + V + \rho_m \right),$$

$$2\dot{H} + 3H^2 = -\kappa^2 \left(\frac{1}{2} \dot{\phi}^2 - V + \omega_m \rho_m \right), \quad (27)$$

and

$$\ddot{\phi} + 3H\dot{\phi} + V_{,\phi} = 0, \quad (28)$$

respectively. Here ρ_m and ω_m are the energy density and the equation of state for the matter sources. In this section, we also consider the case of dust matter, $\omega_m = 0$.

Observing Eqs. (27) and Eq. (28), we could absorb the constant $\kappa^2/3$ ($\kappa^2 = 8\pi$) into ϕ^2 , V and ρ_m , respectively,

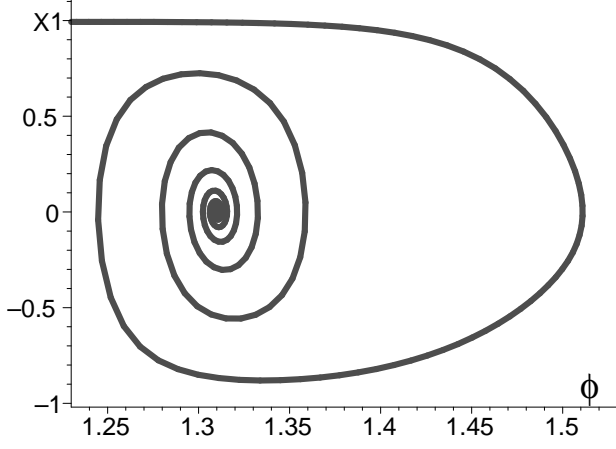


FIG. 3: Evolution of the speed ($X = \dot{\phi}$) of generalized DBI field with ϕ . The point ($\phi = \sigma_2 = 1.31$, $X = 0$) is a stable spiral and thus an attractor. In this case, the generalized DBI field behaves as a damping oscillator in the false vacuum (σ_2) and finally is frozen.

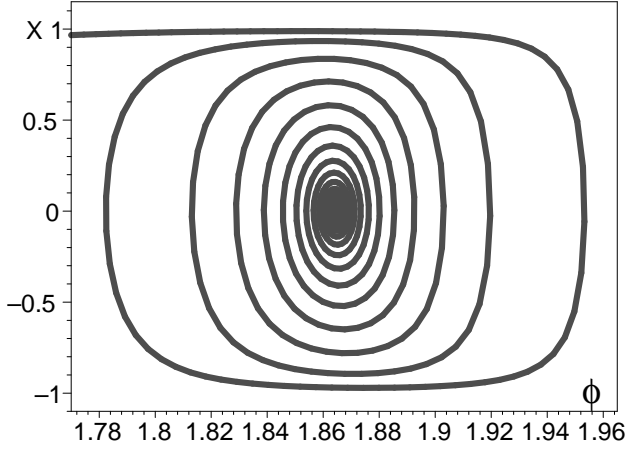


FIG. 4: Evolution of the speed ($X = \dot{\phi}$) of generalized DBI field with ϕ . The point ($\phi = \sigma_2 = 1.86$, $X = 0$) is a stable spiral and thus an attractor. In this case, the generalized DBI field behaves as a damping oscillator in the real vacuum (σ_3) and finally is frozen.

$$\phi^2 \longrightarrow \phi^2 \cdot \frac{6}{\kappa^2}, \quad (29)$$

$$V \longrightarrow V \cdot \frac{3}{\kappa^2}, \quad (30)$$

$$\rho_m \longrightarrow \rho_m \cdot \frac{3}{\kappa^2}. \quad (31)$$

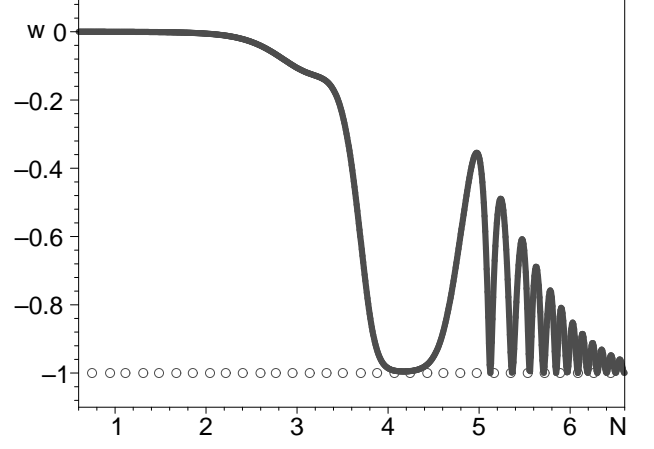


FIG. 5: The evolution of the equation of state for the generalized DBI scalar field. It behaves as the dust matter at higher redshifts and oscillating approaches -1 at the lower redshifts

Then above equations of motion turns out to be

$$H^2 = \dot{\phi}^2 + V + \rho_m, \quad (32)$$

$$2\dot{H}/3 + H^2 = -\dot{\phi}^2 + V - \omega_m \rho_m, \quad (33)$$

$$\ddot{\phi} + 3H\dot{\phi} + \frac{1}{2}V_{,\phi} = 0. \quad (34)$$

Given the scalar potential $V(\phi)$ and the equation of state ω_m , we are left with three variables, $a(t)$, ρ_m and the quintessence $\phi(t)$. Then we have three variables and three independent differential equations. So the system of equations is closed.

The same as the DBI case, it is rather involved to find the analytic solutions to the equations of motion (32-34). Hence in order to solve them numerically, we had better rewrite them in the autonomous form. To our knowledge, one have only explored some special form of the quintessence potential, namely, the exponential potential [12, 20], power-law type potential [9, 13], the Albrecht and Skordis potential [33] and so on. For *arbitrary* potential, one have not yet find a general method to write the equations of motion in the autonomous form. In what follows, we shall propose a method that can be used to deal with *arbitrary* potentials.

To this end, we introduce the following dimensionless quantities

$$X \equiv \frac{\dot{\phi}}{H}, \quad Q \equiv \frac{V_{,\phi}}{V} = Q(Z), \quad (35)$$

$$Y \equiv \frac{\sqrt{V}}{H}, \quad N \equiv \ln a, \quad (36)$$

$$Z \equiv \phi. \quad (37)$$

With the aid of these definitions, we can write the

equations of motion in the autonomous form with *arbitrary* potentials:

$$\begin{aligned}\frac{dX}{dN} &= -3X - Y^2Q - X \cdot \frac{\dot{H}}{H^2}, \\ \frac{dY}{dN} &= \frac{1}{2}XYQ - Y \frac{\dot{H}}{H^2}, \\ \frac{dZ}{dN} &= X,\end{aligned}\quad (38)$$

with

$$\frac{\dot{H}}{H^2} = -3X^2 - \frac{3}{2}(1 + \omega_m)(1 - X^2 - Y^2). \quad (39)$$

We note that Q is the function of Z . Therefore, Eqs. (38) is indeed an autonomous system of equations. In Table II, we present the properties of the five fixed points for the quintessence. The points (a, c, e) correspond to the false vacua (σ_1 , σ_2) and real vacuum (σ_3). The three points are stable spirals. On these epoches, the quintessence behaves as a damping oscillator with the equation of state of firstly behaving as the dust matter and then oscillating approaching -1 . The points (b, d,) correspond to the two local maximum (ξ_1 , ξ_2) and they are saddle points. On these points, the speed of the scalar field exactly vanishes and the quintessence acquires the equation of state of cosmological constant.

In Fig. (7-9), we plot the evolution of the rescaled speed, X of the quintessence with ϕ . The figures show that, with the increasing of initial speed, the quintessence is frozen in the first false vacuum, the second false vacuum and the real vacuum, respectively. Compared to evolution of DBI field, we see from Figs.(2-4) that the DBI field has more times of oscillations than quintessence. How to understand this point? The equations of motion tell us the friction term due to Hubble expansion is $3H\dot{\phi}$ and $3H\dot{\phi}(1 - \dot{\phi}^2)$ for quintessence and DBI field, respectively. Then with the increasing of speed $\dot{\phi}$, the friction term of DBI field is greatly decreased. So the DBI field acquires more times of oscillations.

IV. CONCLUSION AND DISCUSSION

In general, the equations of motion for generalized DBI field and quintessence are rather complicated. So one resort to the method of phase analysis by writing the equations of motion in the autonomous form. Many special form of potentials have been studied for DBI field [29] and quintessence [12–14, 19–28]. However, the general method for dealing with *arbitrary* potentials have not yet been proposed. Thus the outcome of this article is that we have found the method.

Different from the potentials studied in Refs. [12–14, 19–29], we investigate the cosmic evolution of the generalized DBI field and quintessence with the potential of multiple vacua. We find that, with the increasing of

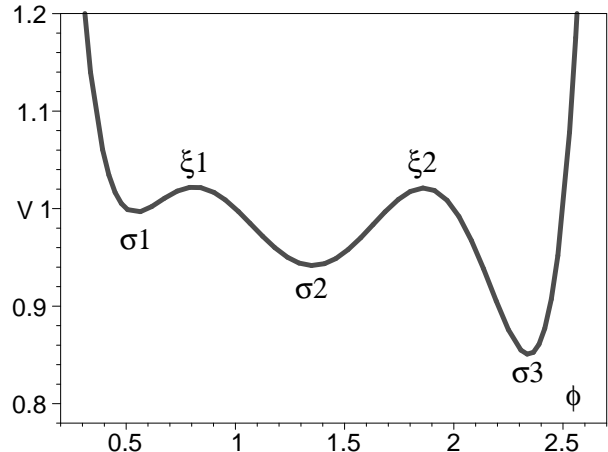


FIG. 6: The quintessence potential $V(\phi)$ with respect to ϕ . There are two local maximum ($\xi_1 = 0.813$, $\xi_2 = 1.862$), one real vacuum ($\sigma_3 = 2.342$) and two false vacuum ($\sigma_1 = 0.545$, $\sigma_2 = 1.355$) for the potential. Physically, the quintessence would firstly damped oscillates between these vacua and finally dwell on one of the vacuum due to the Hubble friction.

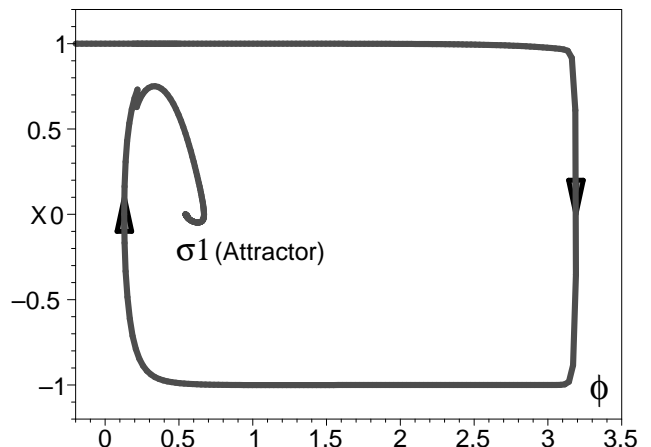


FIG. 7: Evolution of the rescaled speed (X) of quintessence with ϕ . The point ($\phi = \sigma_1$, $X = 0$) is a stable spiral and thus an attractor. The quintessence is finally frozen at $\phi = \sigma_1$.

initial speed, both generalized DBI field and quintessence are successively frozen, in the first false vacuum, the second false vacuum and the real vacuum, respectively. Compared to the evolution of quintessence, the generalized DBI field has more times of oscillations. The reason for this point is that, with the increasing of speed $\dot{\phi}$, the friction term of generalized DBI field is greatly decreased.

Name	X	Y	Z	ϕ	Stability	Ω_ϕ	w_ϕ
(a)	0	1	0.545	$\sigma_1 = 0.545$	Stable spiral (attractor)	1	-1
(b)	0	1	0.813	$\xi_1 = 0.813$	Saddle point	1	-1
(c)	0	1	1.355	$\sigma_2 = 1.355$	Stable spiral (attractor)	1	-1
(d)	0	1	1.862	$\xi_2 = 1.862$	Saddle point	1	-1
(e)	0	1	2.342	$\sigma_3 = 2.342$	Stable spiral (attractor)	1	-1

TABLE II: Properties of the critical points for the quintessence potential given by Eq. (26).

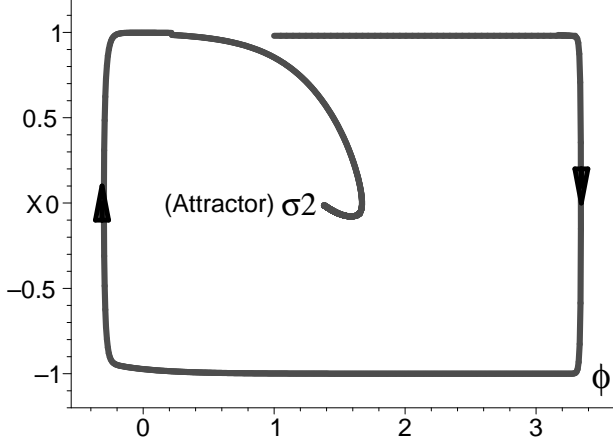


FIG. 8: Evolution of the rescaled speed (X) of quintessence with ϕ . The point ($\phi = \sigma_2$, $X = 0$) is a stable spiral and thus an attractor. The quintessence is finally frozen at $\phi = \sigma_2$.

Thus the generalized DBI field acquires more times of oscillations.

The conclusion in this paper may be trivial, but the proof and the method are not. As an example, one could study the Coleman-De Luccia tunnelling using this method. After making the Wick rotation, $t = -i\tau$ in Eqs. (21) and Eqs. (38), we are able to study the Coleman-De Luccia tunnelling numerically but exactly.

Acknowledgments

We thank one of the referees for pointing out some important typos. This work is supported by the Chinese MoST 863 program under grant 2012AA121701, the NSFC under grant 11373030, 10973014, 11373020 and 11465012.

-
- [1] C. Brans and R. H. Dicke, Phys. Rev. D **124**, 925 (1961).
 - [2] C. Csaki, M. Graesser, L. Randall, J. Terning, Phys. Rev. D **62**, 045015 (2000).
 - [3] P. W. Higgs, Phys. Lett. B **12**, 132 (1964).
 - [4] G. W. Gibbons, K. Maeda, Nucl. Phys. B **298**, 741 (1988).
 - [5] A. Sen, JHEP. **0204**, 048 (2002).
 - [6] S. Thomas and J. Ward, Phys. Rev. D **76**, 023509 (2007) [arXiv:hep-th/0702229]; S. Thomas and J. Ward, JHEP. **0610**, 039 (2006) [arXiv:hep-th/0508085].
 - [7] A. H. Guth, Phys. Rev. D **23**, 347 (1981).
 - [8] Y. Fujii, Phys. Rev. D **26**, 2580 (1982); L. H. Ford, Phys. Rev. D **35**, 2339 (1987); C. Wetterich, Nucl. Phys. B **302**, 668 (1988).
 - [9] B. Ratra and P. J. E. Peebles, Phys. Rev. D **37**, 3406 (1988).
 - [10] T. Chiba, N. Sugiyama and T. Nakamura, Mon. Not. R. Astron. Soc. **289**, L5 (1997).
 - [11] P. G. Ferreira and M. Joyce, Phys. Rev. Lett. **79**, 4740 (1997); Phys. Rev. D **58**, 023503 (1998).
 - [12] E. J. Copeland, A. R. Liddle and D. Wands, Phys. Rev. D **57**, 4686 (1998).
 - [13] R. R. Caldwell, R. Dave and P. J. Steinhardt, Phys. Rev. Lett. **80**, 1582 (1998).
 - [14] I. Zlatev, L. M. Wang and P. J. Steinhardt, Phys. Rev. Lett. **82**, 896 (1999).
 - [15] S. Tsujikawa, Class. Quant. Grav. **30**, 214003 (2013).
 - [16] T. Chiba, T. Okabe and M. Yamaguchi, Phys. Rev. D **62**, 023511 (2000).
 - [17] C. Armendariz-Picon, V. F. Mukhanov and P. J. Steinhardt, Phys. Rev. Lett. **85**, 4438 (2000); Phys. Rev. D **63**, 103510 (2001).
 - [18] R. R. Caldwell, Phys. Lett. B **545**, 23 (2002).
 - [19] A. de la Macorra and G. Piccinelli, Phys. Rev. D **61**, 123503 (2000).
 - [20] S. C. C. Ng, N. J. Nunes and F. Rosati, Phys. Rev. D **64**, 083510 (2001).
 - [21] P. S. Corasaniti and E. J. Copeland, Phys. Rev. D **67**, 063521 (2003).
 - [22] R. R. Caldwell and E. V. Linder, Phys. Rev. Lett. **95**, 141301 (2005).
 - [23] E. V. Linder, Phys. Rev. D **73**, 063010 (2006); E. Elizalde, A. N. Makarenko et al., Astrophys. Space Sci. **344**, 479 (2013).

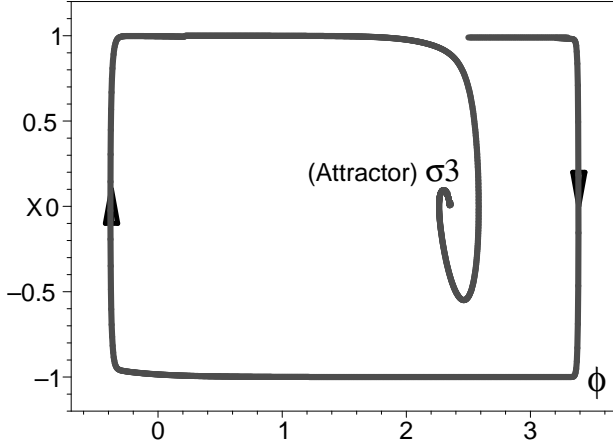


FIG. 9: Evolution of the rescaled speed (X) of quintessence with ϕ . The point ($\phi = \sigma_3$, $X = 0$) is a stable spiral and thus an attractor. The quintessence is finally frozen at $\phi = \sigma_3$.

- [24] T. Barreiro, E. J. Copeland and N. J. Nunes, *Phys. Rev. D* **61**, 127301 (2000).
- [25] E. J. Copeland, S. Mizuno, M. Shaeri, *Phys. Rev. D* **79**, 103515 (2009) [arXiv:0904.0877]; S. Nojiri, S. D. Odintsov, *Phys. Lett. B* **649**, 440 (2007).
- [26] A. R. Liddle and R. J. Scherrer, *Phys. Rev. D* **59**, 023509 (1999).
- [27] V. Sahni, A. Starobinsky, *Int. J. Mod. Phys. D* **9**, 373 (2000); L. A. Urena-Lopez, T. Matos, *Phys. Rev. D* **62**, 081302 (2000); S. A. Pavluchenko, *Phys. Rev. D* **67**, 103518 (2003).
- [28] V. Sahni, L.-M. Wang, *Phys. Rev. D* **62**, 103517 (2000) [astro-ph/9910097]; C. R. Fadrakas, G. Leon, E. N. Saridakis, *Class. Quant. Grav.* **31**, 075018 (2014).
- [29] Z. K. Guo and N. Ohta, *JCAP* **0804**, 035 (2008) [arXiv:0803.1013]; J. Martin and M. Yamaguchi, *Phys. Rev. D* **77**, 123508 (2008); B. Gumjudpai and J. Ward, *Phys. Rev. D* **80**, 023528 (2009); H. Wei, *Phys. Lett. B* **682**, 98 (2009); C. Ahn, C. Kim, E. V. Linder, *Phys. Lett. B* **684**, 181 (2010); E. J. Copeland, S. Mizuno, M. Shaeri, *Phys. Rev. D* **81**, 123501 (2010); K. Tomi, W. Danielle, Z. Ivonne, *JCAP* **06**, 036 (2014).
- [30] R. C. Myers, *JHEP* **9912**, 022 (1999) [arXiv:hep-th/9910053]; A. A. Tseytlin, *Nucl. Phys. B* **501**, 41 (1997) [arXiv:hep-th/9701125].
- [31] M. R. Douglas, *JHEP* **0305**, 046 (2003); S. Ashok and M. Douglas, *JHEP* **0401**, 060 (2004); L. Susskind, [arXiv:hep-th/0302219].
- [32] S. R. Coleman, *Phys. Rev. D* **15**, 2929 (1977); S. R. Coleman, F. De Luccia, *Phys. Rev. D* **21**, 3305 (1980).
- [33] A. Albrecht and C. Skordis, *Phys. Rev. Lett.* **84**, 2076 (1999).